



Technical Note

Development of an open-source GUI computer program for modelling irradiation of multi-segmented phantoms using grid-based system for PHITS

Hiroshi Watabe ^{a,1}, Kwan Ngok Yu ^{b,1}, Nursel Safakatti ^c, Mehrdad Shahmohammadi Beni ^{a,b,*}^a Division of Radiation Protection and Safety Control, Cyclotron and Radioisotope Center, Tohoku University, 6-3 Aoba, Aramaki, Aoba-ku, Sendai, Miyagi, 980-8578, Japan^b Department of Physics, City University of Hong Kong, Tat Chee Avenue, Kowloon Tong, Hong Kong, China^c Graduate School of Biomedical Engineering, Tohoku University, Sendai, 980-8579, Japan

ARTICLE INFO

Article history:

Received 1 August 2022

Received in revised form

28 August 2022

Accepted 30 August 2022

Available online 5 September 2022

Keywords:

Monte Carlo method

Open-source software

PHITS

Ionizing radiation

Multi-segmented phantoms

ABSTRACT

The Monte Carlo (MC) method has become an indispensable part of the nuclear radiation research field. Several widely used and well-known MC packages were developed for simulation of radiation transport and interaction with matter. All these MC packages require users to prepare an input script. The input script can become lengthy for complex models. The process of preparing these input scripts is time-consuming and error-prone. In the present work, we have developed an open-source GUI computer program for modelling radiation transport and interaction in multi-segmented slab phantoms using grid-based system for the widely used PHITS MC package. The developed tools would be useful for future users of PHITS MC package and particularly inexperienced users. The present program is distributed under GPL license and all users can freely download, modify and redistribute the program without any restrictions.

© 2022 Korean Nuclear Society, Published by Elsevier Korea LLC. This is an open access article under the CC BY license (<http://creativecommons.org/licenses/by/4.0/>).

1. Introduction

The use of multi-segmented (homogenous or inhomogeneous) targets in radiation therapy was found to be promising, particularly when studying the interaction of radiation and activation of materials in biological targets [1–5]. These multi-segmented slabs were found to be useful in a variety of applications, such as radiation dosimetry, range verification and validation, benchmarking numerical models etc., as they tended to resemble the layered structure of the human body. Previously, Attanasi et al. [1] employed a five-segment slab phantom to study the dose distribution and yield of positron produced by impinging protons. In another study, Jia et al. [6] modelled a six-segment slab head phantom to evaluate energy deposition and the production of

secondary particles in proton therapy. The modelling of heterogeneous slab phantom in radiation dosimetry has also been performed [7], which is another type of multi-segmented slab phantom. Studies involving multi-segmented phantoms show the importance of using these models in investigating interactions of ionizing radiation with matter.

There are several well-established Monte Carlo (MC) packages being widely used for modelling radiation interaction and transport in matter. Some well-known MC packages are; Monte Carlo N-Particle (MCNP) (<https://mcnp.lanl.gov/>), Geant4 (<https://geant4.web.cern.ch/>), FLUKA (<http://www.fluka.org/fluka.php>) and the Particle and Heavy Ion Transport code System (PHITS) (<https://phits.jaea.go.jp/>). These MC packages have their own specific syntaxes for preparing the input script. In addition, as the complexity of the modelled system increases, the length of the input script would also increase. The preparation of lengthy input scripts would be tedious, time-consuming and error-prone for both new and experienced users. Recently, we have developed a GUI program for simulation of positron emitting radioisotopes which makes the modelling task easier for the users [8]. Considering the multi-

* Corresponding author. Division of Radiation Protection and Safety Control, Cyclotron and Radioisotope Center, Tohoku University, 6-3 Aoba, Aramaki, Aoba-ku, Sendai, Miyagi, 980-8578, Japan.

E-mail address: mehrdad.shahmohammadi.beni.d5@tohoku.ac.jp (M. Shahmohammadi Beni).

¹ Authors contributed equally.

segmented phantoms, preparation of their input script would be particularly tedious, mainly due to the presence of multiple domains with different sizes and material compositions.

In the present work, we have developed an open-source graphical user interface (GUI) program for PHITS MC package for modelling the irradiation of complex multi-segmented (i.e., inhomogeneous) phantoms. Using the present program, no scripting would be required, which helps users simulate multiple irradiation scenarios in an interactive manner in a few seconds. The present program and the developed method would be useful for students and researchers in the field of radiation physics, protection and therapy.

2. Materials and methods

The present program has two main parts, namely, the (1) GUI and (2) script maker module. The GUI was developed using QT5 (<https://www.qt.io/>) libraries and written in C++ programming language, having ~4200 lines of code. The script maker module was written using FORTRAN90 programming language, having ~1000 lines of code. The program uses a grid (i.e., mesh) based system to enable users to model multi-segmented rectangular parallelepiped (i.e., slab) phantoms. The grid size was set to be 10×20 and meshed using squares with user-defined length. The number of segments (i.e., domains) would be defined by the user. Using the grid-based method developed in the present work, users can choose the location of different segments by defining segment number on the 10×20 grid and define the mesh size. The grid-based system has a similar concept as meshing geometries using finite sized elements. The concept of grid-based system is shown schematically in Fig. 1. The segment number would be chosen by the user over the grid and the program automatically assembles these into a seamless domain.

The snapshot of the program in action is shown in Fig. 2. The current version of the program has four different materials that users can choose from, namely, (1) PMMA, (2) water, (3) lung and (4) bone equivalent. Most commonly employed materials in studies involving radiation interaction with biological materials considered water, PMMA, lung, and bone equivalent materials [1]. The densities and material composition are shown in Table 1. The densities and material composition were taken from Refs. [9–11].

There are six different types of ionizing radiation that users can choose using the drop-down menu, namely; (1) proton, (2) neutron, (3) electron, (4) photon, (5) alpha particle and (6) ^{12}C incident beam. The generated phantom will be irradiated using a mono-directional disk source along the positive z-axis. The incident beam energy, source to target distance, ambient air dimension, number of batches (*maxbch*) and histories per batch (*maxcas*), number of tallies and particles to tally are all user-defined through the GUI (see Fig. 2). The program generates inputs for PHITS run based on the inputs from the user. In addition, users can initiate PHITS run using the present program, given that PHITS is installed

on their system with the default system path. The present program was compiled on both GNU/Linux and Microsoft Windows operating systems. We have used GCC compiler package 4.8.5 (<https://gcc.gnu.org/>) to compile the present program. The source code and the Microsoft Windows compatible executable can be downloaded from: https://figshare.com/articles/software/Development_of_an_open-source_GUI_computer_program_for_modelling_irradiation_of_multi-segmented_phantoms_using_grid-based_system_for_PHITS/20408070.

The present program is distributed under GPLv3 license and users can freely download, modify and redistribute the program without any restrictions. We have developed a custom file extension “.inhm” so that users can save their full simulation configurations. Similarly, the the saved .inhm files can be opened in the program GUI; this would be very useful for saving complex models, data sharing and reproducibility between researchers in the field. The program can generate user-defined models in the range of milliseconds, depending on the complexity of the modelled system.

The present program detects those six incident primary particles that are, (1) proton, (2) neutron, (3) electron, (4) photon, (5) alpha particle and (6) ^{12}C using a subroutine and the program would assign T-Deposit tally to score these in the modelled structure. Other particles that would be tallied such as secondary generated radionuclides would be treated as “non-incident particles” in the same subroutine and therefore the program would assign T-Product tally for these secondary radionuclides. Some examples for proton, alpha particle, neutron and electron irradiation of multi-segmented phantoms modelled using the present program are shown in this paper. A total of four different examples were shown, namely, (1) 160 MeV proton irradiation of a 10-segment phantom, (2) 60 MeV alpha particle irradiation of a 4-segment phantom, (3) 0.01 MeV neutron irradiation of a 4-segment phantom and (4) 10 MeV electron irradiation of a 6-segment phantom. All examples, including the generated input codes, the output results and original figures can be downloaded from: https://figshare.com/articles/software/Development_of_an_open-source_GUI_computer_program_for_modelling_irradiation_of_multi-segmented_phantoms_using_grid-based_system_for_PHITS/20408070.

3. Results and discussion

To demonstrate the capability of the present program, four different examples were used. The results of 160 MeV proton irradiation of a 10-segment phantom are shown in Fig. 3. The dose deposition from primary protons and secondary alpha particles were tallied over the modelled 10-segment phantom. During the interaction of protons with the modelled phantom, secondary alpha particles would be generated as a result of $^{16}\text{O}(p,\alpha)^{13}\text{N}$ and $^{14}\text{N}(p,\alpha)^{11}\text{C}$ nuclear reaction. The variation in the dose deposition at the interface of materials in this multi-segmented phantom can be clearly seen in Fig. 3. The variations in the deposited dose by

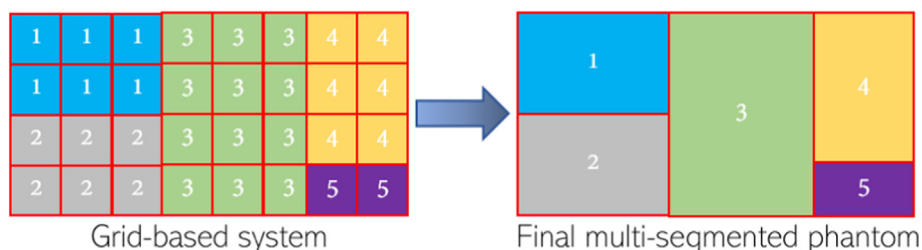


Fig. 1. Schematic representation of grid-based system and final assembly into a multi-segmented phantom.

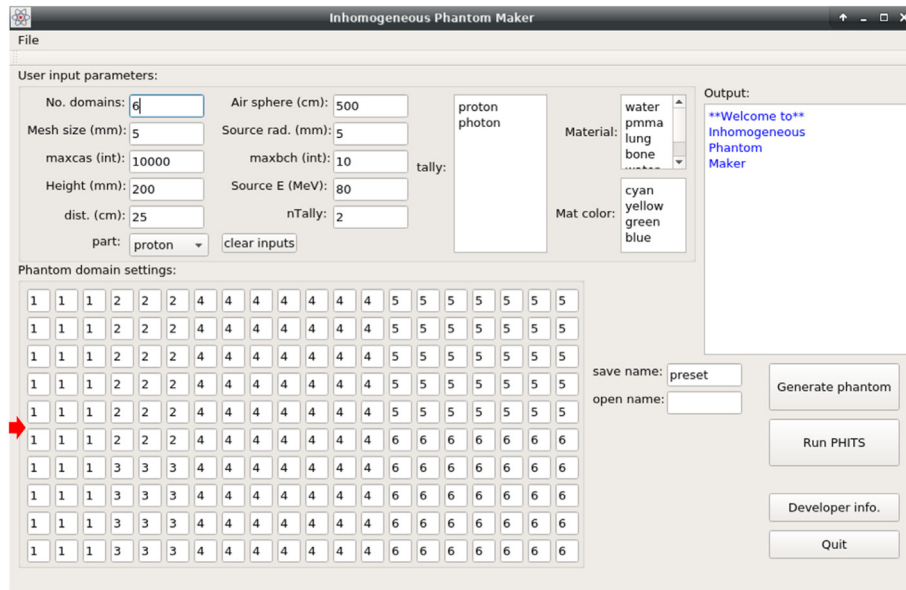


Fig. 2. The developed GUI of the present program in action on GNU/Linux system. The arrow shows the center and the direction of the source.

Table 1
Densities and material compositions (shown in weight percent) used in the present program.

Material	Density (gcm ⁻³)	¹ H	¹² C	¹⁴ N	¹⁶ O	²³ Na	²⁴ Mg	³¹ p	³² S	⁴⁰ Ca
Water	1.000	11.10	-	-	88.90	-	-	-	-	-
PMMA	1.180	8.050	59.99	-	31.96	-	-	-	-	-
Lung equivalent	0.2600	10.30	10.50	3.100	74.90	0.2000	-	0.2000	0.3000	-
Bone equivalent	1.8500	3.400	15.50	4.200	43.50	0.1000	0.1000	10.30	0.3000	22.50

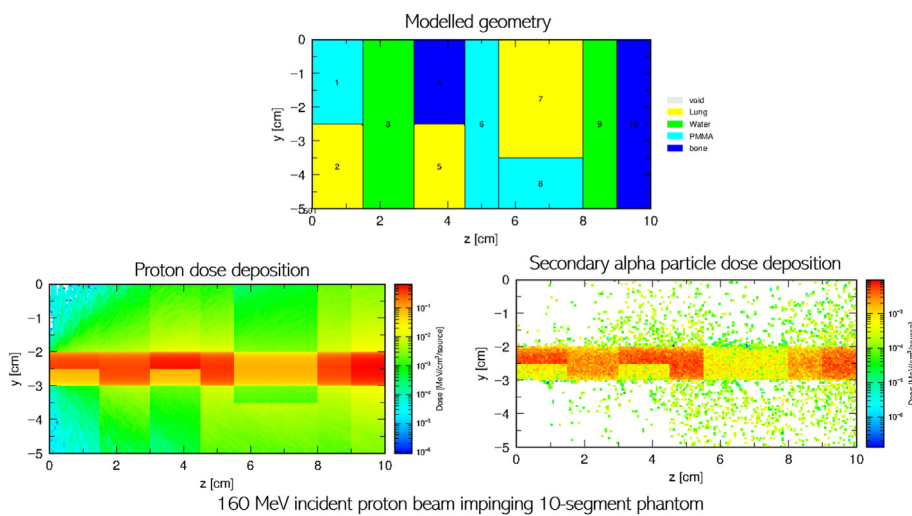


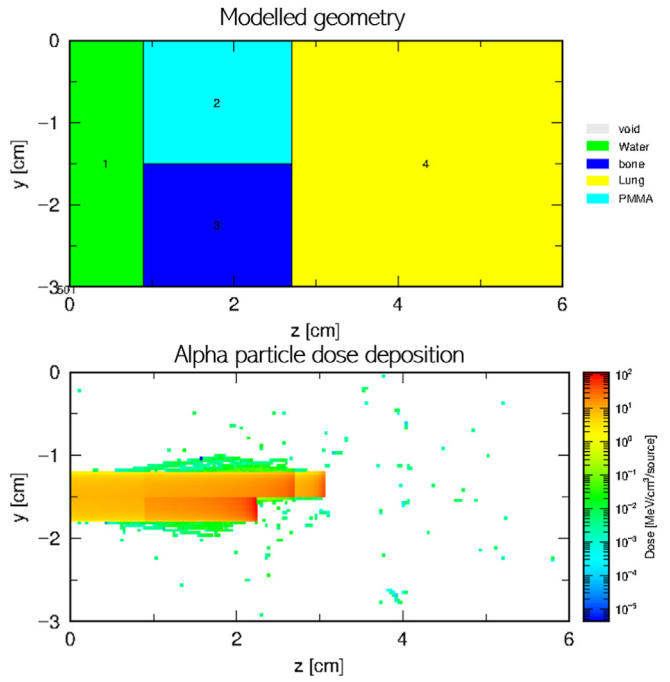
Fig. 3. Irradiation of a 10-segment phantom using 160 MeV incident proton beam. The contour plot shows the dose deposition of primary protons and secondary alpha particles over the modelled phantom. (Note: The height of the phantom was set to be 20 cm).

primary protons and secondary alpha particles are mainly due to changes in the density, material composition and the size of each segment.

The next example reveals the results from 60 MeV alpha particle irradiation of a 4-segment phantom as shown in Fig. 4. From the results of alpha particle irradiation, it can be noted that at the interface between PMMA (segment 2) and bone equivalent (segment 3), the alpha particle dose deposition splits into two

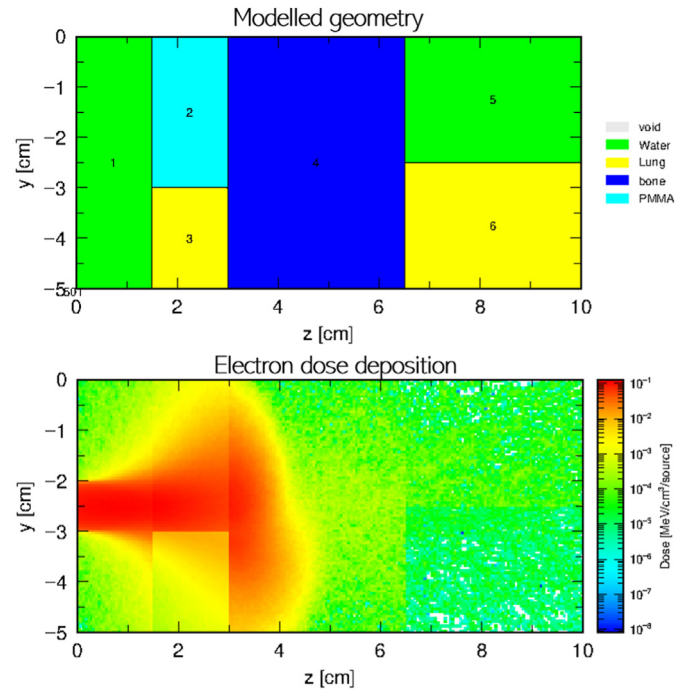
parts; this is mainly due to the fact that the bone equivalent material has higher density and stopping power when compared to PMMA. Therefore, alpha particles stop at lower depth in segment 3 when compared to segment 2.

Another example gives the results from 0.01 MeV neutron irradiation of a 4-segment phantom as shown in Fig. 5. The 4-segment phantom used in this example has a similar arrangement as shown in Fig. 4 but with different dimensions. The



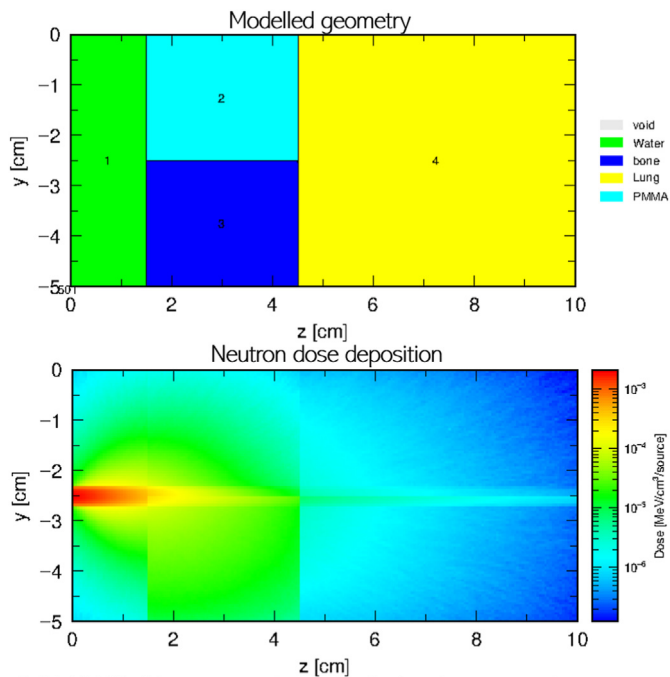
60 MeV incident alpha particle beam impinging 4-segment phantom

Fig. 4. Irradiation of a 4-segment phantom using a 60 MeV alpha particle beam. The contour plot shows the dose deposition of alpha particles over the modelled phantom. (Note: The height of the phantom was set to be 10 cm).



10 MeV incident electron beam impinging 6-segment phantom

Fig. 6. Irradiation of a 6-segment phantom using a 10 MeV electron beam. The contour plot shows the dose deposition of electrons over the modelled phantom. (Note: The height of the phantom was set to be 20 cm).



0.01 MeV incident neutron beam impinging 4-segment phantom

Fig. 5. Irradiation of a 4-segment phantom using a 0.01 MeV neutron beam. The contour plot shows the dose deposition of neutrons over the modelled phantom. (Note: The height of the phantom was set to be 10 cm).

variation in the neutron dose in different segments can be seen in Fig. 5. A smaller beam radius of 0.2 cm was used in this example, that exhibits the behavior of a pencil beam. The neutron beam passes through the water segment, then splits into two parts at the

interface between PMMA and bone equivalent in segments 2 and 3, respectively. The variation of neutron dose deposition at the interface between PMMA and bone equivalent is more subtle when compared to the densely ionizing and charged protons and alpha particles shown in Figs. 3 and 4, respectively. This is mainly due to the fact that neutrons are indirectly ionizing, and they do not have a discrete range in matter unlike protons and alpha particles. The deposited neutron dose tends to reduce with depth as the neutron fluence and energy decrease after propagating through the segments of the modelled phantom and spreads over the tallied region.

The last example which we have used to demonstrate the capabilities of the present program is the irradiation of a 6-segment phantom with a 10 MeV electron beam. The results from this irradiation are shown in Fig. 6. The variation of electron dose can be seen clearly at the interface between PMMA and lung equivalent material in segments 2 and 3, respectively. The spreading of the electron beam, which is mainly due to scattering of electrons, can also be observed. As a result of the interface between PMMA and lung equivalent segments, the spreading of dose deposition in segment 4 (i.e., bone equivalent) exhibits a rather asymmetric distribution; this is mainly due to the difference in the stopping power of electrons in PMMA and lung equivalent material in segments 2 and 3, respectively.

4. Conclusion

The examples shown in the present work demonstrate the capability of the present program in modelling the irradiation of multi-segmented phantoms. The use of grid-based method that was developed and implemented in our program was found to be successful in modelling complex inhomogeneities and interfaces between each segment. Complex geometrical features can be

modelled, thanks to the grid-based system introduced in this work. One must break the complex geometry into smaller segments (similar to the concept of meshing) and assign appropriate materials to these segments. We encourage the readers to download configuration files and examples for some complex geometries that we have modelled from the same download link provided in this paper. The developed program would be a useful tool for future investigators. In future versions of this program, we aim to add a larger material pool for the users.

Data availability

All source codes, executable programs, example files, output files and all original figures can be downloaded from: https://figshare.com/articles/software/Development_of_an_open-source_GUI_computer_program_for_modelling_irradiation_of_multi-segmented_phantoms_using_grid-based_system_for_PHITS/20408070.

Declaration of competing interest

The authors declare that they have no known competing financial interests or personal relationships that could have appeared to influence the work reported in this paper.

Acknowledgment

The present work was supported by the Special Grant for the Development of Virtual Teaching and Learning (VTL) no. 6430120 from the University Grants Committee of Hong Kong and also by the JSPS KAKENHI grant number 21F21103.

References

- [1] F. Attanasi, A. Knopf, K. Parodi, H. Paganetti, T. Bortfeld, V. Rosso, A. Del Guerra, Extension and validation of an analytical model for in vivo PET verification of proton therapy—a phantom and clinical study, *Phys. Med. Biol.* 56 (2011) 5079–5098.
- [2] N. Kholghi, M. Pouladian, A.S. Monfared, Evaluating the accuracy of electron pencil beam dosimetry based on Monte Carlo simulations using homogeneous and heterogeneous phantoms, *Inform. Med. Unlocked* 31 (2022), 101006.
- [3] B. Habib, B. Poumarede, F. Tola, J. Barthe, Evaluation of PENFAST—A fast Monte Carlo code for dose calculations in photon and electron radiotherapy treatment planning, *Physica Med.* 26 (2010) 17–25.
- [4] R. Doucet, M. Olivares, F. DeBlois, E.B. Podgorsak, I. Kawrakow, J. Seuntjens, Comparison of measured and Monte Carlo calculated dose distributions in inhomogeneous phantoms in clinical electron beams, *Phys. Med. Biol.* 48 (2003) 2339–2354.
- [5] O.P. Gurjar, R.K. Paliwal, S.P. Mishra, A dosimetric study on slab-pine-wood-slab phantom for developing the heterogeneous chest phantom mimicking actual human chest, *J. Med. Phys.* 42 (2017) 80–85.
- [6] S.B. Jia, M.H. Hadizadeh, A.A. Mowlavi, M.E. Loushab, Evaluation of energy deposition and secondary particle production in proton therapy of brain using a slab head phantom, *Rep. Pract. Oncol. Radiother.* 19 (2014) 376–384.
- [7] A. Zaman, M.B. Kakakhel, A. Hussain, A comparison of Monte Carlo, anisotropic analytical algorithm (AAA) and Acuros XB algorithms in assessing dosimetric perturbations during enhanced dynamic wedged radiotherapy deliveries in heterogeneous media, *J. Radiother. Pract.* 18 (2019) 75–81.
- [8] M. Shahmohammadi Beni, K.N. Yu, M.R. Islam, H. Watabe, Development of PHITS graphical user interface for simulation of positron emitting radioisotopes production in common biological materials during proton therapy, *J. Radiat. Res.* 63 (2022) 385–392.
- [9] E.H. Bentefour, T. Shikui, D. Prieels, H.M. Lu, Effect of tissue heterogeneity on an in vivo range verification technique for proton therapy, *Phys. Med. Biol.* 57 (2012) 5473–5484.
- [10] K. Parodi, A. Ferrari, F. Sommerer, H. Paganetti, Clinical CT-based calculations of dose and positron emitter distributions in proton therapy using the FLUKA Monte Carlo code, *Phys. Med. Biol.* 52 (2007) 3369–3387.
- [11] D.H. Kim, S. Cho, K. Jo, E. Shin, C.S. Hong, Y. Han, T.S. Suh, D.H. Lim, D.H. Choi, Proton range verification in inhomogeneous tissue: treatment planning system vs. measurement vs. Monte Carlo simulation, *PLoS ONE* 13 (2018), e0193904.